Progress in Materials Science 100 (2019) 170–186

Contents lists available at ScienceDirect

Progress in Materials Science

journal homepage: www.elsevier.com/locate/pmatsci

Thermal conductivity of 2D nano-structured boron nitride (BN) and its composites with polymers

Valentina Guerra, Chaoying Wan, Tony McNally*

International Institute for Nanocomposite Manufacturing (IINM), WMG, University of Warwick, CV4 7AL, UK

ARTICLE INFO

Keywords:
Thermal conductivity
2D boron nitride
Composites
Polymers

ABSTRACT

High thermal conductivity, structural stability, good mechanical and anti-oxidant properties makes hexagonal boron nitride (h-BN) a promising functional filler for polymers to produce composite materials where excellent thermal management is required, such as in electronic devices. Theoretical studies have revealed that two dimensional (2D) BN has higher thermal conductivity (up to 400 $Wm^{-1} K^{-1}$, in-plane) than bulk h-BN due to a reduction in phonon-phonon scattering when scaling down the thickness of the material. For this reason, 2D boron nitride nanosheets (BNNS) are gaining intense interest since they could be utilised in the design of composite materials with excellent efficiency to dissipate heat. Various methods have been explored to produce 2D BNNS including mechanical and chemical exfoliation of pristine bulk BN, chemical reaction, chemical vapour deposition (CVD) and electron irradiation. To facilitate the dispersion of BNNS in polymers, different functionalization strategies have been applied for surface-treatment of BNNS. In this review, the different synthesis approaches adopted for BNNS are compared and the effects of BNNS dispersion on the thermal conduction of polymers are discussed. The factors influencing the mechanism of thermal conduction such as materials crystallinity, filler geometry, filler surface functionalization and alignment, filler/matrix interface and processing conditions are discussed. Some perspectives and future directions on how to generate high thermally conductive composites of BNNS and polymer are proposed.

1. Introduction

There continues to be growing interest in the study of boron nitride (BN) as a functional filler for polymers due to its extraordinary properties including high thermal conductivity, structural stability, mechanical properties and anti-oxidation ability [1–15]. BN is a refractory chemical compound, produced synthetically since it is not found in nature. It consists of equal number of boron (B) and nitrogen (N) atoms and is isoelectronic to similar carbon structures. BN exists in various crystalline forms: the hexagonal form (h-BN) is analogous to graphite, the cubic form (c-BN) is isostructural to diamond and the amorphous form (a-BN) is similar to amorphous carbon.

h-BN and graphite are similar in structure since both present layered sp^2-bonded hexagonally packed sheets. However, in graphite the valence electrons are set in a conjugated system that makes it an electron conductor, while in BN the presence of two atoms with very different electronegativity (boron = 2.04, nitrogen = 3.04) gives it partial ionic character, conferring to BN electron insulating properties [2,16]. This structural difference is also reflected in the optical properties of 2D materials, in that, BN is transparent or white if in bulk quantities [17–22] while graphite is black. Moreover, the arrangement of the layers in the two materials is different,

* Corresponding author.
E-mail address: t.mcnally@warwick.ac.uk (T. McNally).

https://doi.org/10.1016/j.pmatsci.2018.10.002
Received 13 November 2017; Received in revised form 7 September 2018; Accepted 20 October 2018
Available online 24 October 2018

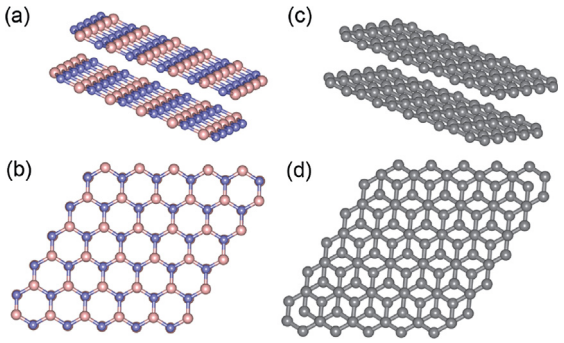

Fig. 1. h-BN (a) and graphite (c) layer structural models. h-BN layers are perfectly overlapped (AA′ stacking) and it is not possible distinguish a top layer from one underneath (b). Graphite layers present a Bernal structure (AB stacking) and it is possible to distinguish the upper layer from a layer below (d). Reprinted from [23] with permission of The Royal Society of Chemistry.

in BN the sheets are in "registry" with the atoms of each layer eclipsed by the atoms of the upper and lower layers, while in graphite the layers are stacked according to a Bernal sequence (AB) [23]. Fig. 1 shows the difference between h-BN and graphite layer arrangement and Table 1 lists the main properties of BN and graphite. Experimentally, the thermal conductivity of graphene has been reported to be as high 5000 Wm/K, depending on the method employed and, theoretically using molecular dynamics to be as high as 10,000 Wm/K [24–26].

h-BN can be exfoliated and shaped in different nanostructures such as 2D BN nanosheets (BNNS) [18,28–31] and BN spherical nanoparticles (BNNP) [32,33]. It is also possible to synthetize BN nanotubes (BNNT) from h-BN [34–38] by air plasma treatment or chemical vapour deposition (CVD). BN nanostructures may be used as fillers to produce white or transparent [39] highly thermally conductive and electrically insulating polymer composites. However, the high BNNT surface tension (26.7 mN/m) and the high interfacial thermal resistance between the nanotubes and the matrix [40–43] make it more difficult to adhere to the polymer matrix [44–46] compared to BNNS.

This review is focused on the thermal conductivity of BN in both sheet and flake form, the former having a 2D nanostructure and the latter having at least one dimension on the nanoscale and, when either are a functional filler for polymeric materials. In particular, the synthesis and properties of BNNS are described, with focus on the intrinsic thermal conductivity of BNNS and the translation of this property to polymers.

2. Synthesis and characterization of BN

2.1. Mechanical exfoliation

BNNS were first obtained by mechanical exfoliation or cleavage, a technique developed in 2004 [47]. It relies on the use of an adhesive tape to peel off BN layers which are successively attached onto a substrate such as Si/SiO_2. The layers obtained can be easily viewed under the optical microscope. Unfortunately, this procedure does not allow a few BN layers to be harvested, because of the strong lip-lip interactions between BN planes that stabilize the multi-layered structure [48,49]. BN nanosheets with thickness between 3.5 and 80 nm have been obtained [48]. Additional shearing treatment may help break the Van der Waals interactions among the BN layers. A ball milling process was firstly applied to BN by Li et al. in 2011 [50]. In order to reduce the impact and associated attrition of the balls and contamination, a milling agent has to be used (e.g. benzyl benzoate, $C_{14}H_{12}O_2$). Fig. 2 shows the SEM images of the nanosheets obtained using this technique and a schematic illustrating the action of the ball on the BNNS.

Table 1
Comparison of properties between hexagonal boron nitride and graphite [27]. Reprinted from J. Mat. Sci. Technol., 31, Jiang XF, Weng QH, Wang XB, Li X, Zhang J, Golberg D, et al. Recent Progress on Fabrications and Applications of Boron Nitride Nanomaterials: A Review, 589–98, Copyright (2015), with permission from Elsevier.

Properties	*h*-BN	*h*-graphite
Bond length (nm)	0.144	0.142
Bond energy (eV)	4	3.7
Interlayer spacing, by diffraction (nm)	0.333	0.335
Young's modulus (TPa)	0.81–1.3	1.1
In-Plane thermal conductivity (W/mK)	400	2600
Charge transferred between neighbors (e)	~0.4	~0
Band gap (eV)	5.5–6.0	~0
Breakdown voltage (MV/cm)	~7	Conductor
Oxidation resistance (°C)	~840	~600
Appearance color	White/near-transparent	Black

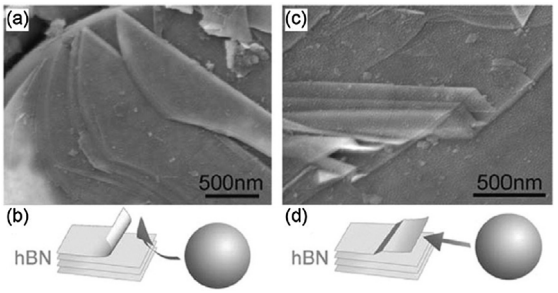

Fig. 2. SEM images of BNNS obtained by ball milling (a) and (c) the mechanism of action of the balls during milling (d) and (e). Reprinted from [23] with permission of The Royal Society of Chemistry.

2.2. Chemical exfoliation (Sonication)

Han et al. [29] first prepared mono-and-few layered BNNS by means of sonication of an organic dispersion containing h-BN crystals. Different organic solvents such as N,N-dimethylformamide (DMF), chloroform, 1,2-dichloroethane and methanesulfonic acid (MSA) [23] have been used. The combination of sonication and strong interactions between the solvent and BN surfaces permits exfoliation of the layers. The use of hydroxides like sodium hydroxide (NaOH) and potassium hydroxide (KOH) may assist layer separation. The adsorption of cations (Na^+ or K^+) on the outer BN surfaces leads to curling of the surfaces that allows the anions (OH^-) to penetrate between the layers, causing further curling of the layers and finally, adsorption and reaction between BN and anions induces the layers to be peeled away from each other [23]. Sonication allows for sheets with thickness between 2 and 10 nm to be collected [23,49]. The chemical exfoliation process is shown schematically in Fig. 3.

2.3. Wet chemical reaction

BNNS can also be synthesised through the reaction of [51] boric acid (H_3BO_3) and urea ($CO(NH_2)_2$) at 900 °C under a nitrogen flux [48]. The reactions involved are:

$$2H_3BO_3 \rightarrow B_2O_3 + 3H_2O$$

$$CO(NH_2)_2 \rightarrow NH_3 + HNCO$$

$$B_2O_3 + 2NH_3 \rightarrow 2BN + 3H_2O$$

The number of layers can be adjusted by the reaction concentration [2]. For example, the layer thickness reduces with increasing urea concentration.

BNNS were also produced via a template-free solid phase reaction, where $NaBF_4$, NH_4Cl and NaN_3 powders were pressed into pellets at room temperature and reacted in an autoclave at 300 °C for 20 h according to the following reaction. BNNS flakes were obtained by further solution sonication [52].

$$NaBF_4 + 3NH_4Cl + 3NaN_3 \rightarrow BN + NaF + 3NaCl + 4N_2 + 3NH_3 + 3HF$$

Chemical blowing reactions of NH_3BH_3 involves heating at atmospheric pressure from 80 °C to 110 °C to initiate dehydrogenation and to 400 °C to complete dehydrogenation. In this step, hydrogen was evolved from the B—N—H swollen system and the desired BN product obtained by further heating at 1400 °C for 3 h. In a final step, a BN suspension was obtained via a combination of ultra-sonication and centrifugation. The final product has a few layered structure with lateral dimensions of about 100 μm [53,54].

In another approach combustion-annealing processes can be used. By way of example, a viscous gel consisting of H_3BO_3, CH_4N_2O, NaN_3 and NH_4Cl in water was ignited at 600 °C in a muffle furnace. The resulting product was washed with water first and then with

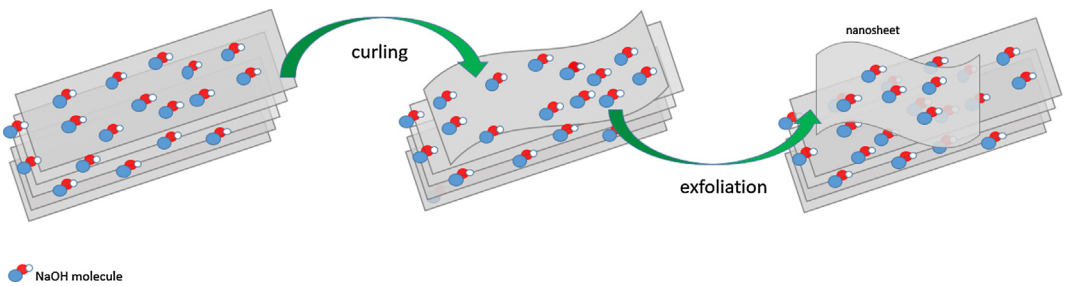

Fig. 3. Schematic representation of BN chemical exfoliation where NaOH molecules first cause curling of the sheets, starting from the edges, then ion penetration among the layers causes exfoliation and the formation of BNNS.

ethyl alcohol, dried in a vacuum and annealed at 1000–1400 °C under nitrogen. With this procedure, it is possible to obtain BN nanoplatelets with a thickness of about 30 nm and lateral sizes of a few hundred nm [55]. BNNS with an average thickness of approximately 4 nm can be prepared from B_2O_3, Zn, $N_2H_4{\cdot}2HCl$ in an autoclave at 500 °C for 12 h then treated with HCl, filtered and dried at 80 °C [56].

A further wet chemistry methodology is via the use of a substitution reaction. A graphite crucible is filled with B_2O_3 powder and covered by molybdenum oxide ((MoO_3) as reaction promoter) and graphene sheets. The reaction is performed at 1650 °C for 30 mins under a nitrogen flux. The product must be taken from the graphene substrate and heated in air at 650 °C for 30 mins in order to remove the graphene residue. The principle of this technique relies on the substitution of an atom (or functional group) in a compound with another atom (group) [57].

2.4. Chemical vapour deposition (CVD)

BNNS can be synthesized by chemical vapour deposition (CVD) techniques starting from different precursors such as BF_3-NH_3, BCl_3-NH_3, borazine ($B_3N_3H_6$), trichloroborazine ($B_3N_3H_6$) or hexachloroborazine ($B_3N_3Cl_6$) [58–66]. Borazine and its compounds are easier to use compared to BF_3-NH_3 and BCl_3-NH_3 since these precursors evolve two or more gases. Borazine ($B_3N_3H_6$) is a compound similar to benzene except the atoms are boron and nitrogen in equal ratio and therefore the two parent atoms of the final products are present in only one precursor. Thus, it is possible to avoid having to use more complicated systems using two or more gaseous precursors.

Using a transition metal such as Pt(1 1 1), Ru(0 0 1), Ni(1 1 1), Cu(1 1 1), Pd(1 1 1), Pd(1 1 0), Fe(1 1 0), Mo(1 1 0), Cr(1 1 0), Rh (1 1 1) [67–78], at high temperature (1000 K) it is possible to synthetize a h-BN monolayer by dehydrogenation of borazine. The product morphology may change according to the different metal used since the interfacial bonding between h-BN and the substrate are different [65]. For example, using Rh(1 1 1) a particular structure called BN nanomesh is formed [67], consisting of a single corrugated layer.

In low-pressure CVD it is possible to use gases produced from BH_3-NH_3 on Cu to obtain h-BN monolayer by nucleation of BN triangle shape islands on the substrate. In fact, at 70–90 °C these little islands grow and merge with each other to form a complete layer on the metal. Low precursor pressure is essential to achieve high quality 2D BN [79]. In 2010 a few layered BN film (about 2–5 layers) was synthetized on Cu by thermal catalytic CVD [20]. A split tube furnace was used to place the substrate at 600 °C for 20 mins under Ar-H_2 flux. Successively BH_3-NH_3 was sublimated at 120–130 °C and carried in the furnace by the Ar-H_2 flux. Large and flat BNNS were obtained if BN and Cu have similar lattice structures.

2.5. Electron irradiation

Jin et al. [80] and Meyer et al. [81] in 2009 first fabricated single layered BNNS by electron irradiation. BN flakes of around 10 layers were firstly mechanically exfoliated then further ‘thinned’ by intensive electron beam irradiation down to a single layer. This method was first used inside a TEM instrument to obtain BN monolayer.

3. Thermal conductivity of BNNS

Table 2 lists the properties of BNNS, including the thermal conductivity of BNNS which has been theoretically and experimentally calculated to be in the range of 300–2000 W/mK and 300–360 W/mK, respectively.

Table 2
Main properties of BNNS.

Characterisation	Properties	References
Colour	Transparent/White	[82]
Bonding	Covalent/ionic	[82]
Electronic structure	5.0–6.0 eV band gap	[82]
Raman	1365–1373 cm^{-1}	[20,83,84]
IR	1370–1378 cm^{-1} in plane B—N stretching; 800–830 cm^{-1} out of plane B—N—B bending	[84–87]
UV	Sharp peak at 203 nm; transparent in the range of 250–900 nm	[20]
XPS	B^xN: 190 BE/eV (B1s); BN^x 398 BE/eV (N1s)	[20,85,88]
XRD	Peak at 2θ = 26; lattice parameters: a = 0.250 nm, c = 0.666 nm; interlayer spacing:0.333 nm	[83,85–87]
Mechanical properties	Elastic Modulus:220–510 Nm^{-2} (thickness about 1–2 nm)	[82]
Thermal conductivity @ RT	300–2000 W/mK (theoretical), 300–360 W/mK (experimental)	[82,89]
Thermal stability	> 600 °C	[82]

3.1. Concept of thermal conductivity

The transfer of the vibrational energy of a particle to an adjacent particle without changing the centre of the mass is thermal conduction. In general, thermal conduction is due to two contributions [90], energized electron motion and phonon conduction, where a phonon is a quantum of vibrational energy. In a metal the former has a major contribution, while in a periodic and elastic system, thermal conduction can be exclusively described in terms of phonons. This property is greatly influenced by material type (i.e. plastics, metals, ceramic), size, binding energy, and morphology (i.e. crystalline structure, atomic density in the network) [90]. The particles on the surface of the material start to vibrate when exposed to a heat source. Subsequently, the heat is transferred to adjacent particles through vibration and, ultimately, through particle vibration throughout the whole material [90].

Thermal conductivity, κ (W/mK) quantifies thermal conduction. When a temperature difference ΔT between two opposite faces of a material is imposed thermal conductivity describes the quantity of heat transferred through a certain thickness of material and along the direction perpendicular to the surface area in a certain time. Thermal conductivity can be determined from [90]:

$$\kappa = \alpha \cdot Cp \cdot \rho \tag{1}$$

where κ is thermal conductivity, C_p is the specific heat at constant pressure, ρ is density and α is thermal diffusivity. It is a measure of the speed of heat transfer (length^2/time). The thermal conductivity (hence thermal conduction) of a material is an intrinsic property of material composition. In Eq. (1), if C_p and ρ are constant, then thermal conductivity is constant. If C_p and ρ of the material change as a function of temperature, then thermal conductivity changes. Additionally, for an isotropic material heat diffuses uniformly whatever the direction, while for an anisotropic material, thermal conductivity depends also on the direction of heat flux. Therefore, thermal conductivity is properly described by a tensor and it is a function of direction and temperature [88]:

$$\kappa_{x,y,z,T} = \begin{pmatrix} \kappa_{xx} & \kappa_{xy} & \kappa_{xz} \\ \kappa_{yx} & \kappa_{yy} & \kappa_{yz} \\ \kappa_{zx} & \kappa_{zy} & \kappa_{zz} \end{pmatrix} \tag{2}$$

The more correct equation for thermal conductivity is therefore:

$$\kappa_{xx}\frac{\delta^2 T}{\delta x^2} + \kappa_{yy}\frac{\delta^2 T}{\delta y^2} + \kappa_{zz}\frac{\delta^2 T}{\delta z^2} + (\kappa_{xy} + \kappa_{yx})\frac{\delta^2 T}{\delta x \delta y} + (\kappa_{yz} + \kappa_{zy})\frac{\delta^2 T}{\delta y \delta z} + (\kappa_{xz} + \kappa_{xy})\frac{\delta^2 T}{\delta x \delta z} = \rho \cdot Cp\frac{\delta T}{\delta t} \tag{3}$$

A numerical model is needed to obtain a solution to Eq. (3) [91–93].

3.2. Thermal conductivity in crystalline materials and polymers

In a crystalline material such as BN, graphene, metals, any discontinuity (i.e. dislocations, point defects, grain boundaries and interfaces) causes a reduction in thermal conductivity, known as Kapitza resistance [94]. Indeed, in a crystalline material the heat propagates through the material as a harmonic wave where all the particles oscillate in the same way at the same frequency. Discontinuity points result in heterogeneity in the structure and particles vibrate differently at different frequencies. This anharmonicity leads to a phonon scattering phenomena, causing a reduction of thermal conductivity. The phonon scattering means that the phonons are not transferred as a unique wave anymore and it may happen in different ways [95]: (i) phonon-phonon scattering: in an ideal case, atoms harmonically vibrate during heat flux. However, atoms vibrate at different frequencies and phonons flip their direction causing scattering; (ii) phonon-interface scattering: this type of scattering is due to the presence of interfaces in a material. It is inevitable since all the materials have finite dimensions, namely interfaces and disconnections and, (iii) phonon-defect scattering: this type of scattering occurs when defects are present in the material. Any defect is a barrier to heat flux and results in phonon scattering.

For semi-crystalline polymers, the amorphous phase behaves as structural defects that diffuse heat slowly. Even highly crystalline polymers still contain intrinsic defects (e.g. chain ends, chain folding), the heat propagation in crystals and polymeric materials can be described by the Newton pendulum model, as shown in Fig. 4.

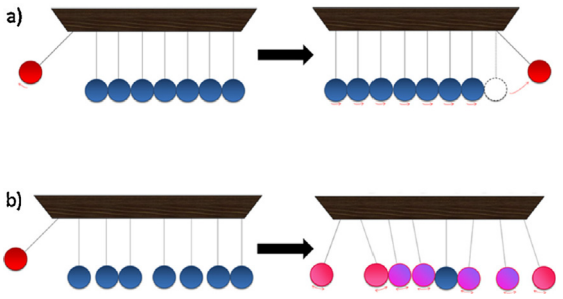

Fig. 4. Newton pendulum model: (a) perfect crystalline material behaviour to heat propagation; (b) polymer behaviour to heat propagation [90]. Reprinted from Prog Polym Sci, 61, Burger N, Laachachi A, Ferriol M, Lutz M, Toniazzo V, Ruch D, Review of thermal conductivity in composites: mechanisms, parameters and theory, 1–28, Copyright (2016), with permission from Elsevier.

As shown in Fig. 4a, a crystalline material is a perfect Newton system where the ordered structure (shown as spheres) facilitates the heat to pass from a particle face to another very quickly without any loss of energy. Conversely, in Fig. 4b, the heat travels through defects in polymers such as the amorphous component and the vibration of the entire chains, causing a disordered oscillation leading to a loss of energy from one particle to another, therefore, most polymers are highly thermally insulating, with κ values in the range 0.2–0.4 $Wm^{-1}\ K^{-1}$.

Agari et al. [96] proposed a mathematical model to describe thermal conductivity of polymer composites:

$$log\kappa = A \cdot V + B \tag{4}$$

where κ is the thermal conductivity of the composite and V is filler content by volume. The A term is related to the limiting effect of thermal conductivity of the polymer on the thermal conductivity of the filler. The B term takes into account the eventual changes in polymer crystallinity upon filler incorporation. The two terms are expressed by Eqs. (5) and (6).

$$A = C_f \cdot \log\left[\frac{\kappa_2}{Cp \cdot \kappa_1}\right] \tag{5}$$

$$B = \log(Cp \cdot \kappa_1) \tag{6}$$

where κ_1 and κ_2 are the thermal conductivity of the polymer matrix and filler respectively. The ease at which a connecting conductive filler path is formed can be expressed by the C_f (> 0) factor and C_p is the specific heat capacity of the polymer. The ratio κ_2/κ_1 in Eq. (5) is defined as the "reduced thermal conductivity of the filler" and indicates how much the thermal conductivity of the filler in the composite is lower than the thermal conductivity of the pure filler. This means that it is not possible for a polymer based composite to have the same ability to dissipate heat of the embedded filler because the polymer acts as a limiting barrier to heat flow [96].

3.3. Thermal conductivity of composites with BN as an additive (filler)

The addition of highly thermally conductive fillers to polymers can improve the thermal conduction of the polymer matrix, including carbon- [97–104], metallic [105–108] and ceramic fillers [109–113]. Among which h-BN with thermal conductivity up to 400 W/mK at room temperature is extremely promising. Theoretical studies suggest that even higher thermal conductivity may be reached if a reduction in phonon-phonon scattering in the 2D layers can be overcome [23]. In fact, the interlayer coupling facilitates out-of-plane vibration and hence phonon scattering. The thermal conductivity decreases from a monolayer to a multilayer structure up to converge to bulk h-BN thermal conductivity when a few layer system is simulated [114]. It is worth noting that the exceptional electrical insulation and thermal conductivity properties of BN make it a highly interesting material for battery applications.

3.3.1. Effect of filler geometry on thermal conductivity

Filler geometry such as lateral dimensions, sheet/layer thickness and aspect ratio all determine the thermal conductivity of BN. In fact, smaller filler particles cause more phonon scattering than larger ones due to the higher density of interfaces. This leads to a reduction of the thermal conductivity [115,116]. Michael Shtein et al. [115] managed to enhance the thermal conductivity of composites of epoxy resins and GNP by adding filler particles having a lateral size of around 20 μm, a thickness of around 10 nm and an aspect ratio of around 1000. The final thermal conductivity was almost four times higher than the pure matrix.

Several workers reported that it is possible to enhance the thermal conductivity of polymers by adding BNNS on the micrometre length scale [117,118]. By way of example, Hatsuo Ishida et al. [117] increased the thermal conductivity of polybenzoaxine up to 30 times higher than the pure matrix, by adding BNNS having a lateral sizes of 225 μm for a loading of 78.5 vol%. Surprisingly, the effect of BNNS geometry on κ has been poorly investigated.

3.3.2. Effect of processing parameters on thermal conductivity

Composites produced by different processes may present different characteristics. Moreover, according to the procedure adopted, defects can be created both on the micro-scale, such as voids and, on the macro-scale such as porosity. Additionally, higher filler loading generally results in increased viscosity in the melt state which can be detrimental since the higher the viscosity, the larger the porosity of the final material [23]. To date, the main processes used for production of composites of polymers and BNNS are sonication [1,2,119,120], ball-milling [121–123], pressing [117,124,125] and mixing [5,126–129]. Each method directly impacts the state of filler dispersion and distribution in the polymer matrix, an important parameter in attaining a composite material with enhanced thermal conductivity.

3.3.3. Effect of BNNS dispersion on thermal conductivity

Achieving effective dispersion of the filler in the polymer matrix is a non-trivial task, since the filler particles, especially on the nanoscale tend to agglomerate due to their high surface energy [130]. Mackay et al. reported that a stable dispersion of molten polymer and nanoparticles forms when the polymer radius of gyration is larger than the nanoparticle radius. For example, in a system made of polystyrene nanoparticles in polystyrene the miscibility occurs when the polystyrene radius of gyration is 1–4 times larger than the nanoparticle radius [131]. It is important to note that the extent of dispersion is not so influential on composite properties at lower filler concentration but it affects composite performance at high filler loadings [132–134]. This may be due to the segregation of the filler in the polymer for very low concentrations [135]. It is also essential to underline that thermal conductivity is more influenced by the interactions between filler particles in the matrix rather than filler content (number of filler particles) [136]. In fact,

a three dimensional thermal network is produced when the level of particle interactions is high, reducing interfacial thermal resistance (ITR) but improving thermal conductivity [136]. Previous studies pointed to the existence of different dispersion states for a 2D platelet like filler in a polymer matrix [137–139], namely separated, intercalated and exfoliated, depending on the technique used to prepare the composites and the affinity between matrix and filler [137,139]. Usually low miscibility and exfoliation leads to the formation of a separated phase consisting of a structure of very large agglomerates of filler. The intercalated phase still presents a stacked structure but with major interlayer spacing (few nm) than the separated one. Finally, in the exfoliated configuration the filler is well dispersed in the polymer and the sheets have the largest surface area and hence aspect ratio.

Effective dispersion is a fundamental requirement to achieve improved thermal conductivity of a polymer matrix on addition of BN since an interconnected touching network of BN particles is required so as to create an optimal thermal path through the matrix via particle-particle connectivity [135]. It is important to highlight that higher thermal conductivity is not always obtained by high levels of dispersion. Indeed, the higher the level of dispersion, the more interfaces are created in the system, acting as Kapitza resistance. On the other hand, isolated filler agglomerates are not efficient thermal conductors as a dispersed system at low filler concentration. Presumably, in some cases the interfaces depending on the extent of the dispersion are less detrimental than the large mean inter-particle distances [90]. It is clear the importance of the filler-polymer interface in determining the thermal conductivity of a composite material.

3.3.4. Effect of filler-polymer interface compatibility on thermal conductivity and functionalization methods of BNNS

Filler-polymer compatibility impacts on all composite properties which in turn is determined by chemical composition, filler concentration and geometry of the particle (shape and size) and in some instances filler alignment [139,140].

Naskar et al. [141] stated that in order to improve the properties of composites it is essential to create a continuous phase where the polymer is immobilized on the nanoparticle surfaces. For example, they report that a continuous phase on the micrometre-scale can be reached when both graphene nanoplatelets (GNPs) and carbon nanotubes (CNTs) are added to epoxy resin, improving mechanical properties. This is due to an enhancement of polymer/filler adhesion by adding an inclusive material (graphene in this case) that reduces the distance between the polymer and the filler, in effect the interface. Fig. 5 shows the difference between a discontinuous and a continuous phase.

By reducing the interface between polymer and filler it is also possible to improve the thermal conductivity of composites. Large interfaces, in fact, cause phonon scattering [42,142]. Furthermore, the larger the interface region the longer the time for heat dissipation. Therefore, a perfect compatibility has to be reached between filler and matrix in order to reduce the size of the interface and hence phonon scattering. Besides small particle inclusion in the composite as mentioned above, filler surface functionalization is a further methodology utilised to improve filler compatibility with the matrix to achieve high levels of dispersion.

The most common method adopted when functionalizing BNNS is via covalent functionalization, which relies on a chemical reaction with a particular functional group. Hydroxide compounds are used to enhance the mechanical exfoliation of BNNS and also used to functionalize BN, as well as the reaction with other inorganic substances such as acids or peroxides [40,120,143–145]. Organic compounds such as stearic acid derivatives [121], organic acids [110,140,146], isocyanate [147], phenyletilamine [148], alcohols [149], silane derivatives [16,125,150–155] and polysilazane [156] are also alternatives to inorganic acids. Some authors reported *ad hoc* structures synthetized in order to functionalize BN [157] but, usually these structures are amphiphilic compounds having therefore a group that is compatible with the filler and another group compatible with the matrix. In this way, the structure

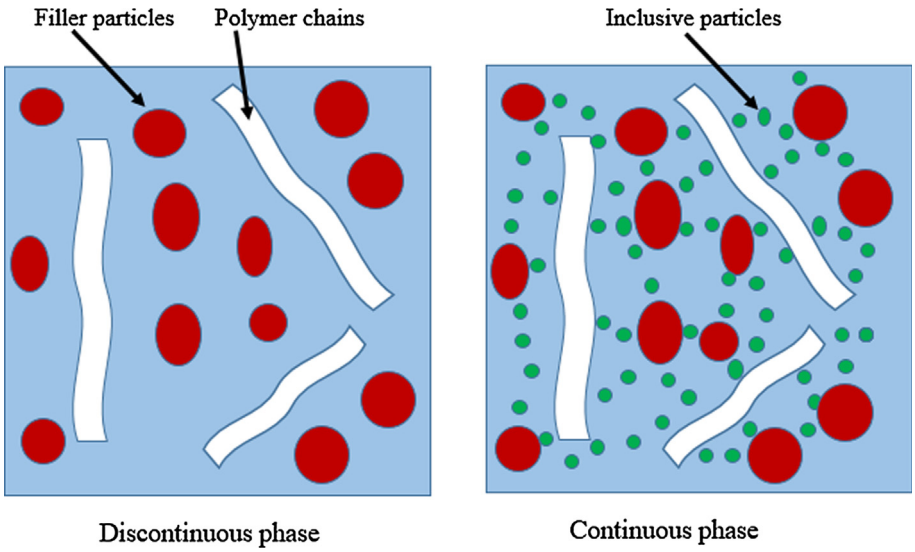

Fig. 5. On the left: filler particles do not adhere onto polymer chain. This increases the polymer/filler interface, which results into a discontinuous phase. On the right: by adding inclusive particle, it is possible to immobilize the polymer chain onto the filler particles. This reduces the polymer/filler interface, which results into a continuous phase by creating a 3D network.

links filler and matrix together.

Silane derivatives are the most used. However, BN is not reactive with silane-based agents. In fact, silane compounds are quite reactive toward hydroxyl groups that are not present in boron nitride [150,158–160] unless in very small quantities depending on the procedure adopted to exfoliate the pristine filler. For this reason, some experiments report a previous BN treatment with a hydroxide and then the filler is further functionalized with a silane compounds such as dimethylsiloxane and 3-ammino-propyl-3-ethoxy-sylane [16,151,152].

Another approach is via a low oxidation route [161] where BNNS at high temperatures in presence of air promotes the introduction of oxygen groups onto the BNNS surface. A similar procedure uses an organic peroxide to facilitate the oxygen radical reaction. The hydroxyl groups formed after reaction with the peroxide are removed by way of hydrolysis [162].

Air plasma treatment is a promising functionalization method since it doesn't involve chemicals, it is relatively simple and allows control of BN wettability and hence adhesion properties [163]. This technique relies on the use of an air flow, made of essentially nitrogen, oxygen and water vapour, undertaking a heating process at high temperatures. This allows oxygen to react with water vapour forming ions such as $[H^+]$, $[O^{2-}]$, and $[OH^-]$ which are very reactive and attack the BN surface. The process starts from BN sheet edges since they are more reactive due to the presence of dandling bonds and followed by reactions inside the BN structure, where defects like vacancies are usually present [163]. The mechanism is very complex and involves different processes such as Lewis acid-base reactions where hydroxyl groups act as acid while boron acts as base. Moreover, the ions may also attack the B—N bond forming new chemical links. The functionalization introduces OH groups which create a wettability gradient on the BN surface depending on how much surface is exposed to the treatment [163]. This is a most interesting result since having control over wetting properties opens up many potential applications in fields such as inkjet printing and surface-directed liquid flow [164–169].

Other workers reported non-covalent functionalization through π-π interactions using compounds containing alkyl amine, alkyl phosphine, and aromatic groups [18,170-172]. Fig. 6 provides a schematic representation of the main functionalization procedures reported to modify BNNS.

3.3.5. *Effect of filler alignment on thermal conductivity*

It is possible by directing filler particles along the same axis in the polymer matrix, to enhance the thermal conductivity of the composite material. For this purpose, tape cast [40], spin-cast [173], shear alignment [174], use of magnetic [146,175–178] or electric fields [179] have been employed to align BNNS. Recently, the application of magnetic fields to align BNNS has aroused an increasing interest since it is possible to control filler particle orientation and direction [180,181]. Fig. 7 shows the alignment of the filler in the polymer matrix when applying a magnetic field [175]. It can be seen that in an ideal configuration the filler is perfectly aligned along the direction of the applied magnetic field (a and b), while in the case of random alignment (c) it is not possible to establish a unique orientation axis:

In order to apply this technique, the filler has to be responsive to the applied magnetic field. Neat BNNS has a low magnetic dipole and therefore was coated with magnetic nanoparticles such as Ni, Fe, Co [182] and Fe_3O_4 [175,180]. The drawback of this approach is related to filler content, if it is too high alignment is hindered by the steric interaction between filler particles [176].

4. BN application as filler in thermoplastic and thermoset based composites

The majority of polymers such as common thermoplastics (e.g. poly(ethylene), poly(propylene), poly(amides)) and thermosets (e.g. epoxy resins) are insulators and have low thermal conductivity but, as described above, this property can be improved by addition of an appropriate filler, such as BN. If the application requires both efficient electric insulation and thermal conduction like

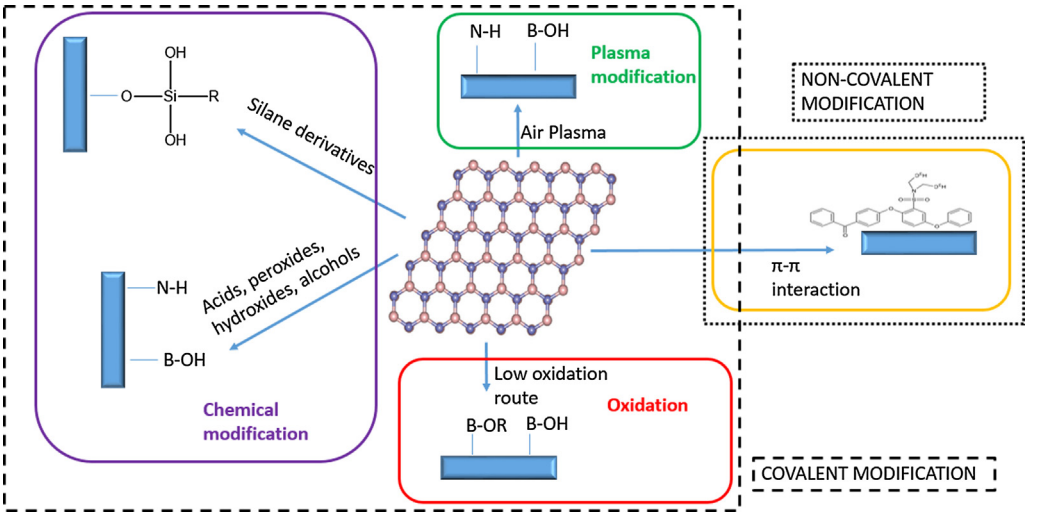

Fig. 6. Methodologies adopted for BNNS functionalization.

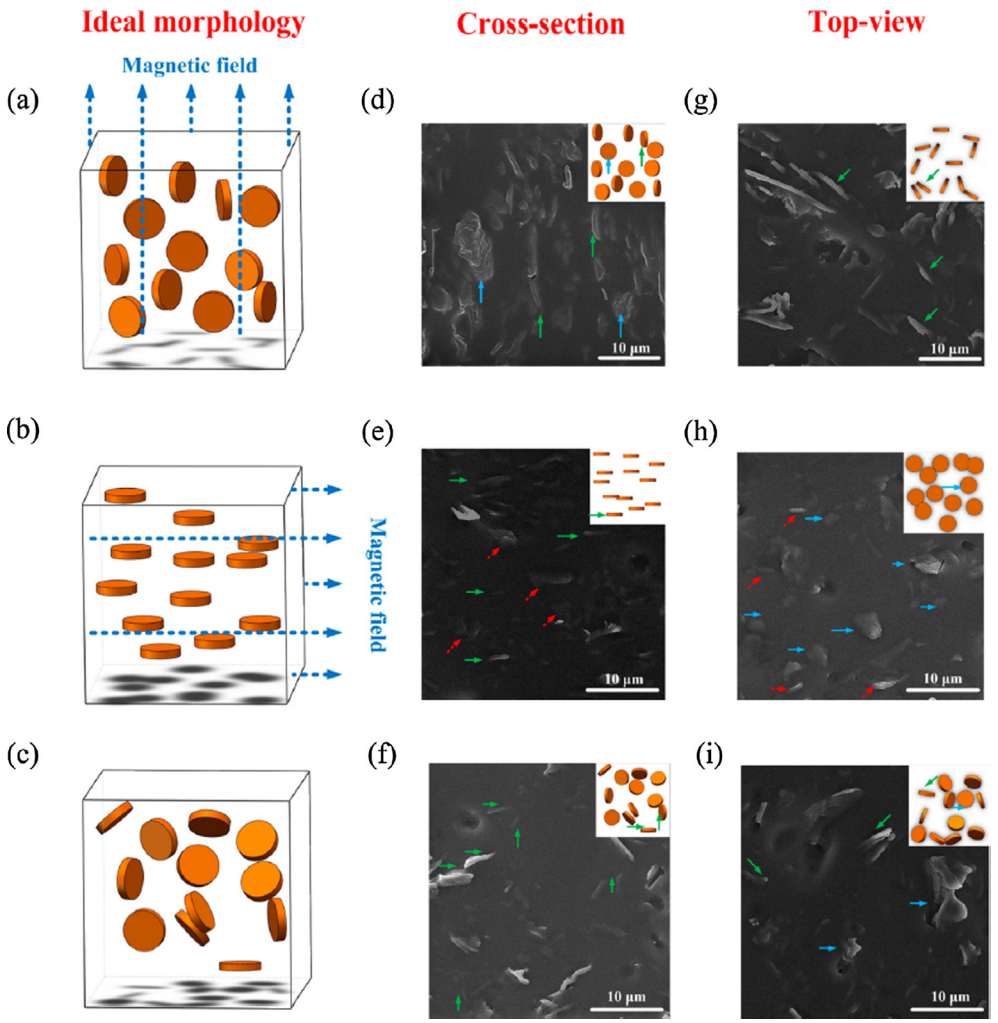

Fig. 7. Alignment along magnetic field axis orientation (a and b) with the corresponding cross-sectional and top view FIB-SEM images (d, g, e, and f). Filler random configuration (c) and corresponding FIB-SEM images (f and i) [175]. Reprinted with permission from Yuan C, Duan B, Li L, Xie B, Huang M, Luo X. Thermal Conductivity of Polymer-Based Composites with Magnetic Aligned Hexagonal Boron Nitride Platelets. ACS Appl Mater Interfaces. 2015;7:13000–6. Copyright (2015) American Chemical Society.

in certain electronic applications, BN filled polymers are one solution [183]. Materials scientists are working hard to find an optimal formulation of BN polymer composite for electronic devices, in order to face the critical challenge of heat dissipation. Normally thermal conduction is the means through which electric devices dissipate the heat produced during their operation [184,185], but if the thermal conductivity of the material which the device is made of is not sufficiently high, then heat is not efficiently dissipated, causing a reduction in the service life of the device.

4.1. Composites of thermoplastic polymers and 2D BN

Composites with thermoplastic polymeric matrices and thermal conductive and (electrically insulating) fillers such as BN are arousing interest.

There are relatively few publications which focus on the study of the thermal conductivity of composites of thermoplastics filled with 2D BN and in many instances the BN filler is not well characterised [124,130,135,147,151,156,186–190] therefore, it is quite difficult to extract the influence of filler (chemical composition, morphology, surface characteristics, shape and size) on thermal conductivity of the system of interest. In other cases [146,151,157,191], very low thermal conductivity values are reported for the final composites (< 1 W/mK) and the results are seldom deeply discussed. In other instances the heat flux mechanism in the final composite is analysed just in terms of the thermal diffusivity [149,157,174] and this is not appropriate since, as explained in the previous sections, thermal conduction is quantified by thermal conductivity and hence thermal diffusivity alone is not informative, see Eq. (3). Moreover, many publications report just the value obtained for thermal conductivity (κ) of the composite of interest and seldom account for other important factors in determining κ, including polymer crystallinity, composite preparation technique and

Table 3
Thermal conductivity values for composites of thermoplastic polymers and BN.

Filler	Matrix	Composite processing procedure	κ (W/mK)	Ref.
BNNS, 23 wt%	PMMA	Solution mixing in chloroform of BNNS and PMMA. Drying @ RT and heating @ 50 °C	2.6	[4]
BNNS, 30 wt% functionalized with hydrogen peroxide by solution mixing	PVA	Magnetic stirring of BN in 8 wt% PVA aqueous solution. Tape-casting on glass panel	4.5	[40]
BN sheets, 30 vol%	PP	Mixing in a batch kneader @ 250 °C, 15 mins. Compression moulding @ 200 °C, 19.6 MPa	2	[190]
BN plates, 50 wt%	SEBS/EVA[1]	Laboratory scale twin-screws compounder @ 200 °C, 100 rpm, 5mins. Compression moulding @ 200 °C, 150 bar, 4 mins	1.6	[189]
BN plates, 30 vol%	HDPE	Mixing in a blender @ RT. Melt press @ 200 °C, 5 MPa, 15 mins	1.2	[135]
BN flakes, 30 vol% functionalized with titanium oxide by sol-gel reaction with sodium hydroxide	Polyurethane acrylate (PUA)	Solution mixing in THF for 5 h. Drying at 80 °C for few hours	2.3	[188]
BN flakes, 0.5 vol%	HDPE	Mixing @ 200 °C, 30 rpm, 20mins. Hot press @ 200 °C, 15 MPa, 30 mins	~5	[186]
BN plates, 30 vol%	PP	Extrusion-Injection moulding (clamping force: 70 ton; cooling time: 10 s; injection rate: 50 cm^3/s; mould T: 40 °C; volume: 49 cm^3; barrel T: 200 °C, 185 °C, 180 °C, 175 °C, 165 °C)	~1.2	[192]
BNNS, 35 vol%	Silicon rubber	Extraction of polymer/filler dispersion in isopropyl alcohol with water. Further treatment with two-roll mill. Final curing with dycumil peroxide @150 °C, 15 MPa	5.47	[118]
BNNS, 15 vol%	Poly(dimethylsiloxane)	Sonication @1500 rpm, 5mins. Filler particles alignment by using a DC electric field (50 Hz) for 16 h	1.6	[179]

[1] SEBS = Styrene-ethylene-butylene-styrene.

cooling regime. Suplicz et al. studied the correlation between change in PP crystallinity and thermal conductivity as a function of BN loading and highlighted the role of melt processing in determining κ [188]. From DSC studies on injection moulded samples, the authors observed that the crystallinity of the composites after the first heating was around 6% lower than pure PP. The authors proposed that the higher thermal conductivity of the composites due to BN inclusion leads to a higher cooling rate in the mould after injection, i.e. the composites cool down quicker than the pure PP, causing the drop in crystallinity in the composites. Similar behaviour was obtained by Radhakrishnan et al. for silica-PP based composites [189]. Moreover, these workers also observed an increase in composite crystallinity relative to unfilled PP for the cooling and the second heating cycle DSC experiments. The authors asserted that the filler acts as a nucleating agent increasing the crystallinity in the final material. However, this effect is evident at low cooling rate as that one used for the DSC analysis; conversely, it obscured at high rate of cooling as that one used in the injection moulding machine. Therefore, having control over the cooling rate when projecting a composite with high thermal conductivity is crucial to ensure the success of the final material performance. As mentioned above A. Suplicz et al. obtained a composite with a thermal conductivity of 1.2 W/mK. Table 3 shows the highest values reported in literature at the time of writing for the thermal conductivity of composites prepared from polymers and BN and the corresponding composite preparation technique adopted.

A typical value of thermal conductivity for BN-filled thermoplastic composites is in the range 1 to 5 W/mK. The highest values of thermal conductivity were obtained by Xie et al. [40] (4.5 W/mK), Shin et al. [186] (~ 5 W/mK) and Kuang et al. (5.47 W/mK). Xie et al. associated their value for composite thermal conductivity to the alignment of the filler in the matrix by applying a magnetic field during the processing. Shin et al. assigned their results to the reduction of the thermal resistance at filler/matrix interface with increasing filler particle size (BNNS lateral size = 20 μm). Kuang et al. [118] proposed that the thermal conductivity obtained was a consequence of the high levels of orientation of the filler in the matrix achieved via an oscillatory shearing of the composite on a two-roll mill.

4.2. Composites of thermosetting polymers and 2D BN

Among thermoset polymers, epoxy resins are widely used due to their excellent chemical resistance, adhesion and mechanical properties [193]. However, epoxy resins have very low thermal conductivity values (0.15–0.35 W/mK) [194] which limits their application in fields where heat dissipation is crucial (e.g. in electronic devices and CFRP tooling).

Researchers have focused on thermoset-based composites filled with BN in order to enhance the thermal conductivity of the matrix polymer. In some cases, the thermal conductivity is quite low (< 1 W/mK) [1,144,145,153,195,196]. Researchers have achieved higher thermal conductivity values by using different shapes of BN, such as BN particles [125] (10.31 W/mK) or BN aggregates and whiskers [143]. It is evident that the geometry of the filler particle plays an important role in determining the thermal conductivity of the composite material. However, the shape of the filler is not always reported in the published literature [116,147,155]. Table 4 lists the highest values reported in literature for the thermal conductivity of composites prepared from thermosets and BN.

As shown in Table 4, the values for thermal conductivity of epoxy resins filled with BN cover a wide range and are achieved at high filler content and, in all instances at filler loadings that are not commercially viable. The highest value (100 W/mK) was obtained by Zhu et al. [119]. The authors proposed that this was due to the functionalization of BNNS with hydroxyl groups after dispersing the filler in isopropyl alcohol. In fact, the presence of hydroxyl groups on BNNS make them chemically compatible with the structure of the wood derived polymer surface used as the matrix.

Other functionalizing agents have been adopted to make BN compatible with polymer matrixes. Kim et al. studied the enhancement of composite thermal conductivity when the BN filler was treated with glycidoxypropyl trimetoxysilane [16], but the value of κ obtained was a factor of ~35 less than that reported in [114]. In fact, the hydroxyl groups of the functionalizing agent improve the interactions between filler and matrix.

It is also interesting to note that Xu et al. [125] who used the same functionalized agent, obtained a value of thermal conductivity almost four times higher than Kim et al. [16], although both used a laser flash method to determine κ. This discrepancy may be associated with the more effective composites preparation process utilized by Xu et al. [125].

Wang et al. [198] achieved a value of 3 W/mK which was associated with improved interfacial interactions between filler and matrix by functionalizing BNNS with silver nanoparticles. The authors proposed that the thermal conductivity of the composite was due to the decreasing thermal resistance between BNNS and matrix by bridging them with silver nanoparticles. Other workers attained enhanced thermal conductivity through the addition of BN having large particle sizes (225 μm) [117], or by aligning the BN particles in polymers in the attempt to create a filler network through which the heat can be efficiently dissipated [173,176,177]. By way of comparison, the thermal conductivity of graphene filled polymers, particularly with epoxy resins has been studied and values of 14 Wm/K have been recorded when the graphene is part of a hybrid filled system [199–201]. Values as high as 90 Wm/K have been reported when graphene was laminated on to poly(ethylene terephthalate) substrates [202].

5. Concluding remarks and future perspectives

The extraordinary properties of 2D BN, including high thermal conductivity combined with structural stability, good mechanical properties and anti-oxidation ability have aroused intense research interest in this material as a functional filler for polymers. Thermal conduction is a complex process and depends on different parameters correlated to both the filler and matrix employed to prepare the composite, including morphology, crystallinity, chemical composition, filler functionalization and level of dispersion in the polymer matrix, filler alignment in the polymer, processing techniques employed to prepare the composite and most importantly

Table 4
Thermal conductivity values for composites of thermosetting polymers and BN.

Filler	Matrix	Composite processing procedure	κ (W/mK)	Ref.
BNNS, 70 wt% functionalized with glycidoxypropyl trimethoxysilane by solution mixing	Epoxy resin	Impregnation of epoxy resin on filler substrate	2.8	[16]
BN flakes, 40 vol% functionalized with iron oxide nanoparticles by solution mixing	Epoxy resin	Magnetic stirring. Degassing @ 50 °C, 1 h. Pressing between two magnets of 0.4 T. Curing @ 120 °C, 3 h	5.5	[177]
BN plates, 20 vol% functionalized with iron oxide nanoparticles by solution mixing	Epoxy resin	Mechanical stirring. Magnetic field exposure by using a rotating magnet (5 Hz)	1.4	[176]
BN plates, 60 vol%	Polyimide	Mixing and curing @ 250 °C	7	[197]
BN flakes, 60 vol%	Polyimide	Spin-cast. Heating @70 °C, and from 70 °C to 350 °C and 220 °C for 2 h	16	[173]
BNNS, 25 vol%, functionalized with silver nanoparticles	Epoxy resin	Stirring for 24 h. Heating from 150 °C to 180^{oC} and 220 °C for 2 h	3	[198]
BN plates, 57 vol%, functionalized with glycidoxypropyl trimethoxysilane by solution mixing	Epoxy resin	Mixing/pressing @ RT. 10.5 MPa, 2 h. Hot press @ 45 °C, 10.5 MPa, 1 h	10.31	[125]
BN flakes, 78.5 vol%	Polybenzoaxine	Mixing @ 80 °C, 10mins. Compression moulding @ 200 °C, 0.1 MPa, 2 h	32.5	[117]
BNNS, 50 wt%, functionalized with isopropyl alcohol by solution mixing	Wood derived polymer	Solution mixing for 10 mins of BN isopropyl alcohol dispersion with polymer water dispersion (previously stirred for 30 mins). Sonication for 15 mins, filtration and drying @ RT	100	[119]
BN plates, 30 wt% functionalized with sulphuric and nitric acid by solution mixing	Epoxy resin	Solution blending of the resin and curing agent @80 °C, 30mins and then cooling @ RT. Sonication of filler and matrix @ 60 °C, 1 h. Curing @ 80 °C, 2 h and postcuring @ 150 °C, 4 h	1.2	[144]

the filler-matrix interface.

Fillers with high aspect ratio and crystallinity are required to improve thermal conductivity of composite materials and achieve a reduction in Kapitza resistance. In this sense, BNNS are interesting, as theoretical studies have shown it has a higher thermal conductivity value than bulk h-BN, due to a reduction in phonon scattering of 2D BN. Typical experimental values for thermal conductivity of BNNS are in the range of 300–360 W/mK [89].

Chemical compatibility between BNNS and the polymer matrix is key to achieving a composite material with significantly enhanced thermal conductivity. The most common routes for chemical functionalization of BNNS have been by using silane agents or via plasma processes. Furthermore, the BNNS must be highly dispersed with the polymer matrix. However, it should be noted that high levels of BNNS dispersion does not imply higher composite thermal conductivity since the greater the extent of dispersion, the higher the interfacial resistance between filler and matrix, leading to a reduction in thermal conductivity. Indeed, even the addition of the most highly thermally conducting filler does not imply that composite materials will have very high thermal conductivity. This behaviour is associated with the resistance of the polymer against the heat flux that results in reduced thermal conductivity. In order to overcome this problem, it is possible to address polymer heat flux by aligning the filler (BNNS) in the matrix in a given direction. In this way, it is possible to create a filler network where the heat flux is efficiently dissipated.

The processing technique used to prepare the polymer-BNNS composites are also very important as different processes may lead to defects in the composite and any defect and discontinuity cause a reduction in thermal conductivity.

Moving forward there are at least three key challenges which must be addressed if high thermal conducting composites of polymers and BNNS are to be fully realised:

(i) BNNS structure and properties: the precursor materials as well as the final BNNS must be fully characterised, in terms of its chemical composition, morphology, surface chemistry and physical properties.
(ii) BNNS – polymer interface: critical to attaining a high thermal conducting composite is the formation of an interconnecting BNNS network throughout the polymer matrix. The BNNS must be touching as to minimise interfacial thermal resistance (ITR) and promote phonon conduction. Different functionalisation strategies are required to knit the BNNS network together within the polymer matrix without degrading the intrinsic thermal conducting properties of BNNS.
(iii) BNNS dispersion: it must be possible to homogeneously disperse BNNS throughout the polymer matrix using industrially relevant processes, e.g. extrusion or compounding with regard thermoplastics and high shear mixing with regard thermosets such as epoxies.

Irrespective of how well BNNS is dispersed in any polymer matrix, if challenge (ii) is not met, then translation of the outstanding thermal conductivity of BNNS to polymer matrices will be very limited.

Acknowledgment

VG thanks the EPSRC (EP/L016389/1) and Thomas Swan Ltd for funding a studentship.

References

[1] Lin Z, McNamara A, Liu Y, Moon K, Wong CP. Exfoliated hexagonal boron nitride-based polymer nanocomposite with enhanced thermal conductivity for electronic encapsulation. Compos Sci Technol 2014;90:123–8.
[2] Kiran MSRN, Raidongia K, Ramamurty U, Rao CNR. Improved mechanical properties of polymer nanocomposites incorporating graphene-like BN: dependence on the number of BN layers. Scripta Mater 2011;64:592–5.
[3] Zhi C, Bando Y, Tang C, Kuwahara H, Golberg D. Large-scale fabrication of boron nitride nanosheets and their utilization in polymeric composites with improved thermal and mechanical properties. Adv Mater 2009;21:2889–93.
[4] Wang X, Pakdel A, Zhang J, Weng Q, Tianyou Z, Zhi C, et al. Large-surface-area BN nanosheets and their utilization in polymeric composites with improved thermal and dielectric properties. Nanoscale Res Lett 2012;7:662.
[5] Jung J, Kim J, Uhm YR, Jeon JK, Lee S, Lee HM, et al. Preparations and thermal properties of micro- and nano-BN dispersed HDPE composites. Thermochim Acta 2010;499:8–14.
[6] Kemaloglu S, Ozkoc G, Aytac A. Properties of thermally conductive micro and nano size boron nitride reinforced silicon rubber composites. Thermochim Acta 2010;499:40–7.
[7] Blase X, Rubio A, Louie SG, Cohen ML. Stability and band-gap constancy of boron-nitride nanotubes. Europhys Lett 1994;28:335–40.
[8] Chen Y, Zou J, Campbell SJ, Le Caer G. Boron nitride nanotubes: pronounced resistance to oxidation. Appl Phys Lett 2004;84:2430–2.
[9] Zettl A, Chang CW, Begtrup G. A new look at thermal properties of nanotubes. Phys Status Solidi B 2007;244:4181–3.
[10] Chang CW, Fennimore AM, Afanasiev A, Okawa D, Ikuno T, Garcia H, et al. Isotope effect on the thermal conductivity of boron nitride nanotubes. Phys Rev Lett 2006;97.
[11] Chang CW, Han WQ, Zettl A. Thermal conductivity of B-C-N and BN nanotubes. Appl Phys Lett. 2005;86.
[12] Chopra NG, Zettl A. Measurement of the elastic modulus of a multi-wall boron nitride nanotube. Solid State Commun 1998;105:297–300.
[13] Hernandez E, Goze C, Bernier P, Rubio A. Elastic properties of C and BxCyNz composite nanotubes. Phys Rev Lett 1998;80:4502–5.
[14] Golberg D, Costa PMFJ, Lourie O, Mitome M, Bai X, Kurashima K, et al. Direct force measurements and kinking under elastic deformation of individual multiwalled boron nitride nanotubes. Nano Lett 2007;7:2146–51.
[15] Suryavanshi AP, Yu MF, Wen JG, Tang CC, Bando Y. Elastic modulus and resonance behavior of boron nitride nanotubes. Appl Phys Lett 2004;84:2527–9.
[16] Kim K, Kim J. Fabrication of thermally conductive composite with surface modified boron nitride by epoxy wetting method. Ceram Int 2014;40:5181–9.
[17] Gorbachev RV, Riaz I, Nair RR, Jalil R, Britnell L, Belle BD, et al. Hunting for monolayer boron nitride: optical and Raman signatures. Small 2011;7:465–8.
[18] Lin Y, Williams TV, Connell JW. Soluble, exfoliated hexagonal boron nitride nanosheets. J Phys Chem Lett 2010;1:277–83.
[19] Kim KK, Hsu A, Jia X, Kim SM, Shi Y, Hofmann M, et al. Synthesis of monolayer hexagonal boron nitride on Cu foil using chemical vapor deposition. Nano Lett 2012;12:161–6.
[20] Song L, Ci L, Lu H, Sorokin PB, Jin C, Ni J, et al. Large scale growth and characterization of atomic hexagonal boron nitride layers. Nano Lett 2010;10:3209–15.

[21] Shi Y, Hamsen C, Jia X, Kim KK, Reina A, Hofmann M, et al. Synthesis of few-layer hexagonal boron nitride. Thin film by chemical vapor deposition. Nano Lett 2010;10:4134–9.
[22] Coleman JN, Lotya M, O'Neill A, Bergin SD, King PJ, Khan U, et al. Two-dimensional nanosheets produced by liquid exfoliation of layered materials. Science 2011;331:568–71.
[23] Pakdel A, Bando Y, Golberg D. Nano boron nitride flatland. Chem Soc Rev 2014;43:934–59.
[24] Balandin AA. Thermal properties of graphene and nanostructured carbon materials. Nat Mater 2011;10:569–81.
[25] Nika DL, Balandin AA. Two-dimensional phonon transport in graphene. J Phys Condens Matter 2012;24.
[26] Nika DL, Balandin AA. Phonons and thermal transport in graphene and graphene-based materials. Rep Prog Phys 2017.;80.
[27] Jiang XF, Weng QH, Wang XB, Li X, Zhang J, Golberg D, et al. Recent progress on fabrications and applications of boron nitride nanomaterials: a review. J Mater Sci Technol 2015;31:589–98.
[28] Golberg D, Bando Y, Huang Y, Terao T, Mitome M, Tang C, et al. Boron nitride nanotubes and nanosheets. ACS Nano 2010;4:2979–93.
[29] Han WQ, Wu LJ, Zhu YM, Watanabe K, Taniguchi T. Structure of chemically derived mono- and few-atomic-layer boron nitride sheets. Appl Phys Lett 2008;93:3.
[30] Lin Y, Williams TV, Cao W, Elsayed-Ali HE, Connell JW. Defect functionalization of hexagonal boron nitride nanosheets. J Phys Chem C 2010;114:17434–9.
[31] Yu J, Qin L, Hao Y, Kuang S, Bai X, Chong YM, et al. Vertically aligned boron nitride nanosheets: chemical vapor synthesis, ultraviolet light emission, and superhydrophobicity. ACS Nano 2010;4:414–22.
[32] Zhi C, Meng W, Yamazaki T, Bando Y, Golberg D, Tang C, et al. BN nanospheres as CpG ODN carriers for activation of toll-like receptor 9. J Mater Chem 2011;21:5219–22.
[33] Tang C, Bando Y, Huang Y, Zhi C, Golberg D. Synthetic routes and formation mechanisms of spherical boron nitride nanoparticles. Adv Funct Mater 2008;18:3653–61.
[34] Chopra NG, Luyken RJ, Cherrey K, Crespi VH, Cohen ML, Louie SG, et al. Boron-nitride nanotubes. Science 1995;269:966–7.
[35] Zhi C, Bando Y, Tang C, Golberg D. Boron nitride nanotubes. Mater Sci Eng R 2010;70:92–111.
[36] Wang JS, Kayastha VK, Yap YK, Fan ZY, Lu JG, Pan ZW, et al. Low temperature growth of boron nitride nanotubes on substrates. Nano Lett 2005;5:2528–32.
[37] Loiseau A, Willaime F, Demoncy N, Schramchenko N, Hug G, Colliex C, et al. Boron nitride nanotubes. Carbon 1998;36:743–52.
[38] Golberg D, Bando Y, Eremets M, Takemura K, Kurashima K, Yusa H. Nanotubes in boron nitride laser heated at high pressure. Appl Phys Lett 1996;69:2045–7.
[39] Zhi C, Bando Y, Tang C, Honda S, Kuwahara H, Golberg D. Boron nitride nanotubes/polystyrene composites. J Mater Res 2006;21:2794–800.
[40] Xie BH, Huang X, Zhang GJ. High thermal conductive polyvinyl alcohol composites with hexagonal boron nitride microplatelets as fillers. Compos Sci Technol 2013;85:98–103.
[41] Marconnett AM, Yamamoto N, Panzer MA, Wardle BL, Goodson KE. Thermal conduction in aligned carbon nanotube-polymer nanocomposites with high packing density. ACS Nano 2011;5:4818–25.
[42] Gojny FH, Wichmann MHG, Fiedler B, Kinloch IA, Bauhofer W, Windle AH, et al. Evaluation and identification of electrical and thermal conduction mechanisms in carbon nanotube/epoxy composites. Polymer 2006;47:2036–45.
[43] Bryning MB, Milkie DE, Islam MF, Kikkawa JM, Yodh AG. Thermal conductivity and interfacial resistance in single-wall carbon nanotube epoxy composites. Appl Phys Lett 2005;87:161909.
[44] Yum K, Yu MF. Measurement of wetting properties of individual boron nitride nanotubes with the Wilhelmy method using a nanotube-based force sensor. Nano Lett 2006;6:329–33.
[45] Lee CH, Drelich J, Yap YK. Superhydrophobicity of boron nitride nanotubes grown on silicon substrates. Langmuir 2009;25:4853–60.
[46] Li LH, Chen Y. Superhydrophobic properties of nonaligned boron nitride nanotube films. Langmuir 2010;26:5135–40.
[47] Novoselov KS, Geim AK, Morozov SV, Jiang D, Zhang Y, Dubonos SV, et al. Electric field effect in atomically thin carbon films. Science 2004;306:666–9.
[48] Charlier JC, Blase X, De Vita A, Car R. Microscopic growth mechanisms for carbon and boron-nitride nanotubes. Appl Phys A 1999;68:267–73.
[49] Pakdel A, Zhi CY, Bando Y, Golberg D. Low-dimensional boron nitride nanomaterials. Mater Today 2012;15:256–65.
[50] Li LH, Chen Y, Behan G, Zhang HZ, Petravic M, Glushenkov AM. Large-scale mechanical peeling of boron nitride nanosheets by low-energy ball milling. J Mater Chem 2011;21:11862–6.
[51] Nag A, Raidongia K, Hembram K, Datta R, Waghmare UV, Rao CNR. Graphene analogues of BN: novel synthesis and properties. ACS Nano 2010;4:1539–44.
[52] Lian G, Zhang X, Tan M, Zhang S, Cui D, Wang Q. Facile synthesis of 3D boron nitride nanoflowers composed of vertically aligned nanoflakes and fabrication of graphene-like BN by exfoliation. J Mater Chem 2011;21:9201–7.
[53] Wang X, Pakdel A, Zhi C, Watanabe K, Sekiguchi T, Golberg D, et al. High-yield boron nitride nanosheets from 'chemical blowing': towards practical applications in polymer composites. J Phys Condens Matter 2012;24:314205.
[54] Wang X, Zhi C, Li L, Zeng H, Li C, Mitome M, et al. “Chemical blowing” of thin-walled bubbles: high-throughput fabrication of large-area, few-layered BN and C-x-BN nanosheets. Adv Mater 2011;23:4072–6.
[55] Zhao Z, Yang Z, Wen Y, Wang Y. Facile synthesis and characterization of hexagonal boron nitride nanoplates by two-step route. J Am Ceram Soc 2011;94:4496–501.
[56] Pacile D, Meyer JC, Girit CO, Zettl A. The two-dimensional phase of boron nitride: few-atomic-layer sheets and suspended membranes. Appl Phys Lett 2008;92:133107.
[57] Han W-Q, Yu H-G, Liu Z. Convert graphene sheets to boron nitride and boron nitride-carbon sheets via a carbon-substitution reaction. Appl Phys Lett 2011;98.
[58] Pierson HO. Boron-nitride composites by chemical vapor-deposition. J Compos Mater 1975;9:228–40.
[59] Rozenberg AS, Sinenko YA, Chukanov NV. Regularities of pyrolytic boron-nitride coating formation on a graphite matrix. J Mater Sci 1993;28:5528–33.
[60] Middleman S. the role of gas-phase reactions in boron-nitride growth by chemical-vapor-deposition. Mater Sci Eng A 1993;163:135–40.
[61] Adams AC. Characterization of films formed by pyrolysis of borazine. J Electrochem Soc 1981;128:1378–9.
[62] Auwarter W, Suter HU, Sachdev H, Greber T. Synthesis of one monolayer of hexagonal boron nitride on Ni(111) from B-trichloroborazine (ClBNH)(3). Chem Mater 2004;16:343–5.
[63] Muller F, Stowe K, Sachdev H. Symmetry versus commensurability: epitaxial growth of hexagonal boron nitride on Pt(111) from B-trichloroborazine (ClBNH)(3). Chem Mater 2005;17:3464–7.
[64] Constant G, Feurer R. Preparation and characterization of thin protective films in silica tubes by thermal-decomposition of hexachloroborazine. J Less Common Met 1981;82:113–8.
[65] Paffett MT, Simonson RJ, Papin P, Paine RT. Borazine adsorption and decomposition at Pt(111) and Ru(001) surfaces. Surf Sci 1990;232:286–96.
[66] Archer NJ. Chemical vapor-deposition. Phys Technol 1979;10:152–61.
[67] Corso M, Auwarter W, Muntwiler M, Tamai A, Greber T, Osterwalder J. Boron nitride nanomesh. Science 2004;303:217–20.
[68] Auwarter W, Kreutz TJ, Greber T, Osterwalder J. XPD and STM investigation of hexagonal boron nitride on Ni(111). Surf Sci 1999;429:229–36.
[69] Huda MN, Kleinman L. h-BN monolayer adsorption on the Ni (111) surface: a density functional study. Phys Rev 2006;74.
[70] Cavar E, Westerstrom R, Mikkelsen A, Lundgren E, Vinogradov AS, Ng ML, et al. A single h-BN layer on Pt(111). Surf Sci 2008;602:1722–6.
[71] Goriachko A, He Y, Knapp M, Over H, Corso M, Brugger T, et al. Self-assembly of a hexagonal boron nitride nanomesh on Ru(0001). Langmuir 2007;23:2928–31.
[72] Preobrajenski AB, Vinogradov AS, Martensson N. Monolayer of h-BN chemisorbed on Cu(111) and Ni(111): the role of the transition metal 3d states. Surf Sci 2005;582:21–30.
[73] Preobrajenski AB, Vinogradov AS, Ng ML, Cavar E, Westerstrom R, Mikkelsen A, et al. Influence of chemical interaction at the lattice-mismatched h-BN/Rh (111) and h-BN/Pt(111) interfaces on the overlayer morphology. Phys Rev 2007;75:245412.
[74] Morscher M, Corso M, Greber T, Osterwalder J. Formation of single layer h-BN on Pd(111). Surf Sci. 2006;600:3280–4.
[75] Corso M, Greber T, Osterwalder J. h-BN on Pd(110): a tunable system for self-assembled nanostructures? Surf Sci. 2005;577:L78–84.

[76] Vinogradov NA, Zakharov AA, Ng ML, Mikkelsen A, Lundgren E, Martensson N, et al. One-dimensional corrugation of the h-BN monolayer on Fe(110). Langmuir 2012;28:1775–81.
[77] Allan MP, Berner S, Corso M, Greber T, Osterwalder J. Tunable self-assembly of one-dimensional nanostructures with orthogonal directions. Nanoscale Res Lett 2007;2:94–9.
[78] Mueller F, Huefner S, Sachdev H. One-dimensional structure of boron nitride on chromium (110) – a study of the growth of boron nitride by chemical vapour deposition of borazine. Surf Sci 2008;602:3467–76.
[79] Sutter P, Lahiri J, Albrecht P, Sutter E. Chemical vapor deposition and etching of high-quality monolayer hexagonal boron nitride films. ACS Nano 2011;5:7303–9.
[80] Jin C, Lin F, Suenaga K, Iijima S. Fabrication of a freestanding boron nitride single layer and its defect assignments. Phys Rev Lett 2009;102.
[81] Meyer JC, Chuvilin A, Algara-Siller G, Biskupek J, Kaiser U. Selective sputtering and atomic resolution imaging of atomically thin boron nitride membranes. Nano Lett 2009;9:2683–9.
[82] Meng WJ, Huang Y, Fu YQ, Wang ZF, Zhi CY. Polymer composites of boron nitride nanotubes and nanosheets. J Mater Chem C 2014;2:10049–61.
[83] Sajjad M, Morell G, Feng P. Advance in novel boron nitride nanosheets to nanoelectronic device applications. ACS Appl Mater Interfaces 2013;5:5051–6.
[84] Chubarov M, Pedersen H, Hogberg H, Filippov S, Engelbrecht JAA, O'Connel J, et al. Boron nitride: a new photonic material. Physica B Condens Matter 2014;439:29–34.
[85] Nazarov AS, Demin VN, Grayfer ED, Bulavchenko AI, Arymbaeva AT, Shin HJ, et al. Functionalization and dispersion of hexagonal boron nitride (h-BN) nanosheets treated with inorganic reagents. Chem Asian J 2012;7:554–60.
[86] Kostoglou N, Polychronopoulou K, Rebholz C. Thermal and chemical stability of hexagonal boron nitride (h-BN) nanoplatelets. Vacuum 2015;112:42–5.
[87] Kostoglou N, Lukovic J, Babic B, Matovic B, Photiou D, Constantinides G, et al. Few-step synthesis, thermal purification and structural characterization of porous boron nitride nanoplatelets. Mater Des 2016;110:540–8.
[88] Jia SL, Wang ZH, Ding N, Wong YLE, Chen XF, Qiu GY, et al. Hexagonal boron nitride nanosheets as adsorbents for solid-phase extraction of polychlorinated biphenyls from water samples. Anal Chim Acta 2016;936:123–9.
[89] Jo I, Pettes MT, Kim J, Watanabe K, Taniguchi T, Yao Z, et al. Thermal conductivity and phonon transport in suspended few-layer hexagonal boron nitride. Nano Lett 2013;13:550–4.
[90] Burger N, Laachachi A, Ferriol M, Lutz M, Toniazzo V, Ruch D. Review of thermal conductivity in composites: mechanisms, parameters and theory. Prog Polym Sci 2016;61:1–28.
[91] Im H, Hwang Y, Moon JH, Lee SH, Kim J. The thermal conductivity of Al(OH)(3) covered MWCNT/epoxy terminated dimethyl polysiloxane composite based on analytical Al(OH)(3) covered MWCNT. Compos A Appl Sci Manuf 2013;54:159–65.
[92] Agrawal A, Satapathy A. Mathematical model for evaluating effective thermal conductivity of polymer composites with hybrid fillers. Int J Therm Sci 2015;89:203–9.
[93] Suplicz A, Hargitai H, Kovacs JG. Methodology development for through-plane thermal conductivity prediction of composites. Int J Therm Sci 2016;100:54–9.
[94] Giri A, Hopkins PE, Wessel JG, Duda JC. Kapitza resistance and the thermal conductivity of amorphous superlattices. J Appl Phys 2015;118.
[95] Shindé SL, Goela JS. High thermal conductivity materials. New York: Springer; 2006.
[96] Agari Y, Ueda A, Nagai S. Thermal-conductivity of a polymer composite. J Appl Polym Sci 1993;49:1625–34.
[97] Afanasov IM, Savchenko DV, Ionov SG, Rusakov DA, Seleznev AN, Avdeev VV. Thermal conductivity and mechanical properties of expanded graphite. Inorg Mater 2009;45:486–90.
[98] Gu JW, Yang XT, Lv ZY, Li N, Liang CB, Zhang QY. Functionalized graphite nanoplatelets/epoxy resin nanocomposites with high thermal conductivity. Int J Heat Mass Transfer 2016;92:15–22.
[99] Yu AP, Ramesh P, Sun XB, Bekyarova E, Itkis ME, Haddon RC. Enhanced thermal conductivity in a hybrid graphite nanoplatelet – carbon nanotube filler for epoxy composites. Adv Mater 2008;20:4740–4.
[100] Nanda J, Maranville C, Bollin SC, Sawall D, Ohtani H, Remillard JT, et al. Thermal conductivity of single-wall carbon nanotube dispersions: role of interfacial effects. J Phys Chem C 2008;112:654–8.
[101] Hauser RA, King JA, Pagel RM, Keith JM. Effects of carbon fillers on the thermal conductivity of highly filled liquid-crystal polymer based resins. J Appl Polym Sci 2008;109:2145–55.
[102] Balandin AA, Ghosh S, Bao WZ, Calizo I, Teweldebrhan D, Miao F, et al. Superior thermal conductivity of single-layer graphene. Nano Lett 2008;8:902–7.
[103] Martin-Gallego M, Verdejo R, Khayet M, de Zarate JMO, Essalhi M, Lopez-Manchado MA. Thermal conductivity of carbon nanotubes and graphene in epoxy nanofluids and nanocomposites. Nanoscale Res Lett 2011;6:610.
[104] Sun XM, Sun H, Li HP, Peng HS. Developing polymer composite materials: carbon nanotubes or graphene? Adv Mater 2013;25:5153–76.
[105] Chung DDL. Materials for thermal conduction. Appl Therm Eng 2001;21:1593–605.
[106] Yao YM, Zeng XL, Guo K, Sun R, Xu JB. The effect of interfacial state on the thermal conductivity of functionalized Al_2O_3 filled glass fibers reinforced polymer composites. Compos A Appl Sci Manuf 2015;69:49–55.
[107] Hammerstroem DW, Burgers MA, Chung SW, Guliants EA, Bunker CE, Wentz KM, et al. Aluminum nanoparticles capped by polymerization of alkyl-substituted epoxides: ratio-dependent stability and particle size. Inorg Chem 2011;50:5054–9.
[108] Ma AJ, Chen WX, Hou YG, Zhang G. The preparation and cure kinetics researches of thermal conductivity epoxy/AlN composites. Polym Plast Technol Eng 2010;49:354–8.
[109] Lee GW, Park M, Kim J, Lee JI, Yoon HG. Enhanced thermal conductivity of polymer composites filled with hybrid filler. Compos A Appl Sci Manuf 2006;37:727–34.
[110] Li TL, Hsu SLC. Enhanced thermal conductivity of polyimide films via a hybrid of micro- and nano-sized boron nitride. J Phys Chem B 2010;114:6825–9.
[111] Yuan FY, Zhang HB, Li XF, Li XZ, Yu ZZ. Synergistic effect of boron nitride flakes and tetrapod-shaped ZnO whiskers on the thermal conductivity of electrically insulating phenol formaldehyde composites. Compos A Appl Sci Manuf 2013;53:137–44.
[112] Firdaus SM, Mariatti M. Fabrication and characterization of nano filler-filled epoxy composites for underfill application. J Mater Sci-Mater El 2012;23:1293–9.
[113] Wu YC, Yu ZQ. Thermal conductivity of in situ epoxy composites filled with ZrB_2 particles. Compos Sci Technol 2015;107:61–6.
[114] Lindsay L, Broido DA. Theory of thermal transport in multilayer hexagonal boron nitride and nanotubes. Phys Rev 2012;85:035436.
[115] Shtein M, Nadiv R, Buzaglo M, Kahil K, Regev O. Thermally conductive graphene-polymer composites: size, percolation, and synergy effects. Chem Mater. 2015;27:2100–6.
[116] Xiang JL, Drzal LT. Investigation of exfoliated graphite nanoplatelets (xGnP) in improving thermal conductivity of paraffin wax-based phase change material. Sol Energy Mater Sol Cells 2011;95:1811–8.
[117] Ishida H, Rimdsuit S. Very high thermal conductivity obtained by boron nitride-filled polybenzoaxine. Thermochim Acta 1998;320:177–86.
[118] Kuang Z, Chen Y, Lu Y, Liu L, Hu S, Wen S, et al. Fabrication of highly oriented hexagonal boron nitride nanosheet/elastomer nanocomposites with high thermal conductivity. Small 2015;11:1655–9.
[119] Zhu H, Li Y, Fang Z, Xu J, Cao F, Wan J, et al. Highly thermally conductive papers with percolative layered boron nitride nanosheets. ACS Nano 2014;8:3606–13.
[120] Xie B-H, Huang X, Zhang G-J. Ultra-flexible polymethyl methacrylate composites induced by sliding of micron-sized hexagonal boron nitride platelets. Ceram Int 2013;39:8543–8.
[121] Hill RF, DaVanzo SP. Enhanced boron nitride composition and polymer based high thermal conductivity molding compound. In: Application EP, editor. US. EP ed. US1997.
[122] Donnay M, Tzavalas S, Logakis E. Boron nitride filled epoxy with improved thermal conductivity and dielectric breakdown strength. Compos Sci Technol 2015;110:152–8.
[123] Camurlu HE, Akarsu E, ArsIan O, Mathur S. Nanocomposite glass coatings containing hexagonal boron nitride nanoparticles. Ceram Int 2016;42:8856–62.

[124] Takahashi S, Imai Y, Kan A, Hotta Y, Ogawa H. Dielectric and thermal properties of isotactic polypropylene/hexagonal boron nitride composites for high-frequency applications. J Alloys Compd 2014;615:141–5.
[125] Xu Y, Chung DDL. Increasing the thermal conductivity of boron nitride and aluminum nitride particle epoxy-matrix composites by particle surface treatments. Compos Interfaces 2000;7:243–56.
[126] Song WL, Wang P, Cao L, Anderson AJ, Meziani MJ, Farr A, et al. Polymer/boron nitride nanocomposite materials for superior thermal transport performance. Angew Chem Int 2012;51:6498–501.
[127] Khan U, May P, O'Neill A, Bell AP, Boussac E, Martin A, et al. Polymer reinforcement using liquid-exfoliated boron nitride nanosheets. Nanoscale 2013;5:581–7.
[128] Duan ZQ, Liu YT, Xie XM, Ye XY. A simple and green route to transparent boron nitride/PVA nanocomposites with significantly improved mechanical and thermal properties. Chin Chem Lett. 2013;24:17–9.
[129] Xie SB, Istrate OM, May P, Barwich S, Bell AP, Khana U, et al. Boron nitride nanosheets as barrier enhancing fillers in melt processed composites. Nanoscale 2015;7:4443–50.
[130] Zhang X, Shen L, Wu H, Guo S. Enhanced thermally conductivity and mechanical properties of polyethylene (PE)/boron nitride (BN) composites through multistage stretching extrusion. Compos Sci Technol 2013;89:24–8.
[131] Mackay ME, Tuteja A, Duxbury PM, Hawker CJ, Van Horn B, Guan ZB, et al. General strategies for nanoparticle dispersion. Science 2006;311:1740–3.
[132] Zhou WY, Wang CF, Ai T, Wu K, Zhao FJ, Gu HZ. A novel fiber-reinforced polyethylene composite with added silicon nitride particles for enhanced thermal conductivity. Compos A Appl Sci Manuf 2009;40:830–6.
[133] Li SS, Qi SH, Liu NL, Cao P. Study on thermal conductive BN/novolac resin composites. Thermochim Acta 2011;523:111–5.
[134] Agari Y, Ueda A, Tanaka M, Nagai S. Thermal-conductivity of a polymer filled with particles in the wide-range from low to superhigh volume content. J Appl Polym Sci 1990;40:929–41.
[135] Zhou W, Qi S, Li H, Shao S. Study on insulating thermal conductive BN/HDPE composites. Thermochim Acta 2007;452:36–42.
[136] Mosanenzadeh SG, Naguib HE. Effect of filler arrangement and networking of hexagonal boron nitride on the conductivity of new thermal management polymeric composites. Compos B – Eng 2016;85:24–30.
[137] Potts JR, Dreyer DR, Bielawski CW, Ruoff RS. Graphene-based polymer nanocomposites. Polymer 2011;52:5–25.
[138] Alexandre M, Dubois P. Polymer-layered silicate nanocomposites: preparation, properties and uses of a new class of materials. Mater Sci Eng R Rep 2000;28:1–63.
[139] Wang M, Yan C, Ma L. Graphene nanocomposites. In: Hu N, editor. Composites and their Properties. InTech; 2012. p. 17–36.
[140] Lee D, Song SH, Hwang J, Jin SH, Park KH, Kim BH, et al. Enhanced mechanical properties of epoxy nanocomposites by mixing noncovalently functionalized boron nitride nanoflakes. Small 2013;9:2602–10.
[141] Naskar AK, Keum JK, Boeman RG. Polymer matrix nanocomposites for automotive structural components. Nat Nanotechnol 2016;11:1026–30.
[142] McNamara AJ, Joshi Y, Zhang ZMM. Characterization of nanostructured thermal interface materials – a review. Int J Therm Sci 2012;62:2–11.
[143] Kim K, Kim M, Kim J. Thermal and mechanical properties of epoxy composites with a binary particle filler system consisting of aggregated and whisker type boron nitride particles. Compos Sci Technol 2014;103:72–7.
[144] Hou J, Li GH, Yang N, Qin LL, Grami ME, Zhang QX, et al. Preparation and characterization of surface modified boron nitride epoxy composites with enhanced thermal conductivity. Rsc Adv 2014;4:44282–90.
[145] Kelkar AD, Tian Q, Yu DM, Zhang LF. Boron nitride nanoparticle enhanced prepregs: a novel route for manufacturing aerospace structural composite laminate. Mater Chem Phys 2016;176:136–42.
[146] Li TL, Hsu SLC. Preparation and properties of thermally conductive photosensitive polyimide/boron nitride nanocomposites. J Appl Polym Sci 2011;121:916–22.
[147] Jin W, Zhang W, Gao Y, Liang G, Gu A, Yuan L. Surface functionalization of hexagonal boron nitride and its effect on the structure and performance of composites. Appl Surf Sci 2013;270:561–71.
[148] Wu HC, Kessler MR. Multifunctional cyanate ester nanocomposites reinforced by hexagonal boron nitride after noncovalent biomimetic functionalization. ACS Appl Mater Interfaces 2015;7:5915–26.
[149] Zhang RC, Sun D, Lu A, Askari S, Macias-Montero M, Joseph P, et al. Microplasma processed ultrathin boron nitride nanosheets for polymer nanocomposites with enhanced thermal transport performance. ACS Appl Mater Interfaces 2016;8:13567–72.
[150] Yung KC, Liem H. Enhanced thermal conductivity of boron nitride epoxy-matrix composite through multi-modal particle size mixing. J Appl Polym Sci 2007;106:3587–91.
[151] Muratov DS, Kuznetsov DV, Il'inykh IA, Burmistrov IN, Mazov IN. Thermal conductivity of polypropylene composites filled with silane-modified hexagonal BN. Compos Sci Technol 2015;111:40–3.
[152] Kim K, Kim M, Hwang Y, Kim J. Chemically modified boron nitride-epoxy terminated dimethylsiloxane composite for improving the thermal conductivity. Ceram Int 2014;40:2047–56.
[153] Yu J, Huang X, Wu C, Wu X, Wang G, Jiang P. Interfacial modification of boron nitride nanoplatelets for epoxy composites with improved thermal properties. Polymer 2012;53:471–80.
[154] Harrison C, Weaver S, Bertelsen C, Burgett E, Hertel N, Grulke E. Polyethylene/boron nitride composites for space radiation shielding. J Appl Polym Sci 2008;109:2529–38.
[155] Huang T, Zeng XL, Yao YM, Sun R, Meng FL, Xu JB, et al. Boron nitride@graphene oxide hybrids for epoxy composites with enhanced thermal conductivity. RSC Adv 2016;6:35847–54.
[156] Ahn K, Kim K, Kim M, Kim J. Fabrication of silicon carbonitride-covered boron nitride/Nylon 6,6 composite for enhanced thermal conductivity by melt process. Ceram Int 2015;41:2187–95.
[157] Ahn HJ, Eoh YJ, Park SD, Kim ES. Thermal conductivity of polymer composites with oriented boron nitride. Thermochim Acta 2014;590:138–44.
[158] Yung KC, Zhu BL, Yue TM, Xie CS. Development of epoxy-matrix composite with both high-thermal conductivity and low-dielectric constant via hybrid filler systems. J Appl Polym Sci 2010;116:518–27.
[159] Kochetov R, Andritsch T, Lafont U, Morshuis PHF, Picken SJ, Smit JJ, et al. Thermal behaviour of epoxy resin filled with high thermal conductivity nano-powders. EIC 2009.524-8.
[160] Chiang TH, Hsieh TE. A study of encapsulation resin containing hexagonal boron nitride (hBN) as inorganic filler. J Inorg Organomet Polym Mater 2006;16:175–83.
[161] Jin H, Li YF, Li XD, Shi ZQ, Xia HY, Xu Z, et al. Functionalization of hexagonal boron nitride in large scale by a low-temperature oxidation route. Mater Lett 2016;175:244–7.
[162] Sainsbury T, Satti A, May P, Wang ZM, McGovern I, Gun'ko YK, et al. Oxygen radical functionalization of boron nitride nanosheets. J Am Chem Soc 2012;134:18758–71.
[163] Pakdel A, Bando Y, Golberg D. Plasma-assisted interface engineering of boron nitride nanostructure films. ACS Nano 2014;8:10631–9.
[164] Xia D, Johnson LM, Lopez GP. Anisotropic wetting surfaces with one-dimesional and directional structures: fabrication approaches, wetting properties and potential applications. Adv Mater 2012;24:1287–302.
[165] Liimatainen V, Sariola V, Zhou Q. Controlling liquid spreading using microfabricated undercut edges. Adv Mater 2013;25:2275–8.
[166] Jokinen V, Leinikka M, Franssila S. Microstructured surfaces for directional wetting. Adv Mater 2009;21:4835–8.
[167] Chu K-H, Xiao R, Wang EN. Uni-directional liquid spreading on asymmetric nanostructured surfaces. Nat Mater 2010;9:413–7.
[168] Chiou N-R, Lui C, Guan J, Lee LJ, Epstein AJ. Growth and alignment of polyaniline nanofibres with superhydrophobic, superhydrophilic and other properties. Nat Nanotechnol 2007;2:354–7.
[169] Kim E, Whitesides GM. Imbibition and flow of wetting liquids in noncircular capillaries. J Phys Chem B 1997;101:855–63.
[170] Wang W, Bando Y, Zhi C, Fu W, Wang E, Golberg D. Aqueous noncovalent functionalization and controlled near-surface carbon doping of multiwalled boron

nitride nanotubes. J Am Chem Soc 2008;130:8144–5.
[171] Zhi C, Bando Y, Tang C, Golberg D. Immobilization of proteins on boron nitride nanotubes. J Am Chem Soc 2005;127:17144–5.
[172] Zhi CY, Bando Y, Tang CC, Xie RG, Sekiguchi T, Golberg D. Perfectly dissolved boron nitride nanotubes due to polymer wrapping. J Am Chem Soc 2005;127:15996–7.
[173] Tanimoto M, Yamagata T, Miyata K, Ando S. Anisotropic thermal diffusivity of hexagonal boron nitride-filled polyimide films: effects of filler particle size, aggregation, orientation, and polymer chain rigidity. ACS Appl Mater Interfaces 2013;5:4374–82.
[174] Song WL, Wang P, Cao L, Anderson A, Meziani MJ, Farr AJ, et al. Polymer/boron nitride nanocomposite materials for superior thermal transport performance. Angewandte Chemie-International Edition 2012;51:6498–501.
[175] Yuan C, Duan B, Li L, Xie B, Huang M, Luo X. Thermal conductivity of polymer-based composites with magnetic aligned hexagonal boron nitride platelets. ACS Appl Mater Interfaces 2015;7:13000–6.
[176] Yuan C, Xie B, Huang M, Wu R, Luo X. Thermal conductivity enhancement of platelets aligned composites with volume fraction from 10% to 20%. Int J Heat Mass Transfer 2016;94:20–8.
[177] Kim K, Kim J. Vertical filler alignment of boron nitride/epoxy composite for thermal conductivity enhancement via external magnetic field. Int J Therm Sci 2016;100:29–36.
[178] Cho HB, Tokoi Y, Tanaka S, Suematsu H, Suzuki T, Jiang WH, et al. Modification of BN nanosheets and their thermal conducting properties in nanocomposite film with polysiloxane according to the orientation of BN. Compos Sci Technol 2011;71:1046–52.
[179] Cho HB, Nakayama T, Suematsu H, Suzuki T, Jiang WH, Niihara K, et al. Insulating polymer nanocomposites with high-thermal-conduction routes via linear densely packed boron nitride nanosheets. Compos Sci Technol 2016;129:205–13.
[180] Lin ZY, Liu Y, Raghavan S, Moon KS, Sitaraman SK, Wong CP. Magnetic alignment of hexagonal boron nitride platelets in polymer matrix: toward high performance anisotropic polymer composites for electronic encapsulation. ACS Appl Mater Interfaces 2013;5:7633–40.
[181] Erb RM, Libanori R, Rothfuchs N, Studart AR. Composites reinforced in three dimensions by using low magnetic fields. Science 2012;335:199–204.
[182] Boussaad S. Hexagonal boron nitride compositions characterized by interstitial ferromagnetic layers, process for preparing, and composites thereof with organic polymers. US2012.
[183] Zhou W, Qi S, An Q, Zhao H, Liu N. Thermal conductivity of boron nitride reinforced polyethylene composites. Mater Res Bull 2007;42:1863–73.
[184] Sim LC, Ramanan SR, Ismail H, Seetharamu KN, Goh TJ. Thermal characterization of Al_2O_3 and ZnO reinforced silicone rubber as thermal pads for heat dissipation purposes. Thermochim Acta 2005;430:155–65.
[185] Xu YS, Chung DDL, Mroz C. Thermally conducting aluminum nitride polymer-matrix composites. Compos A Appl Sci Manuf 2001;32:1749–57.
[186] Shin YK, Lee WS, Yoo MJ, Kim ES. Effect of BN filler on thermal properties of HDPE matrix composites. Ceram Int 2013;39:S569–73.
[187] Muratov DS, Kuznetsov DV, Il'inykh IA, Mazov IN, Stepashkin AA, Tcherdyntsev VV. Thermal conductivity of polypropylene filled with inorganic particles. J Alloys Compd 2014;586:S451–4.
[188] Kim K, Ju H, Kim J. Filler orientation of boron nitride composite via external electric field for thermal conductivity enhancement. Ceram Int 2016;42:8657–63.
[189] Kemaloglu S, Ozkoc G, Aytac A. Thermally conductive boron nitride/SEBS/EVA ternary composites: "processing and characterization". Polym Compos 2009.
[190] Cheewawuttipong W, Fuoka D, Tanoue S, Uematsu H, Iemoto Y. Thermal and mechanical properties of polypropylene/boron nitride composites. Energy Procedia 2013;34:808–17.
[191] Cakmakci E, Kocyigit C, Cakir S, Durmus A, Kahraman MV. Preparation and characterization of thermally conductive thermoplastic polyurethane/h-BN nanocomposites. Polym Compos 2014;35:530–8.
[192] Suplicz A, Szabo F, Kovacs JG. Injection molding of ceramic filled polypropylene: the effect of thermal conductivity and cooling rate on crystallinity. Thermochim Acta 2013;574:145–50.
[193] Dodiuk H, Goodman SH. Handbook of thermoset plastics. 3rd ed San Diego: William Andrew; 2013.
[194] Chen HY, Ginzburg VV, Yang J, Yang YF, Liu W, Huang Y, et al. Thermal conductivity of polymer-based composites: fundamentals and applications. Prog Polym Sci 2016;59:41–85.
[195] Voo R, Mariatti M, Sim LC. Thermal properties and moisture absorption of nanofillers-filled epoxy composite thin film for electronic application. Polym Adv Technol 2012;23:1620–7.
[196] Wu K, Lei C, Yang W, Chai S, Chen F, Fu Q. Surface modification of boron nitride by reduced graphene oxide for preparation of dielectric material with enhanced dielectric constant and well-suppressed dielectric loss. Compos Sci Technol 2016;134:191–200.
[197] Sato K, Horibe H, Shirai T, Hotta Y, Nakano H, Nagai H, et al. Thermally conductive composite films of hexagonal boron nitride and polyimide with affinity-enhanced interfaces. J Mater Chem. 2010;20:2749.
[198] Wang FF, Zeng XL, Yao YM, Sun R, Xu JB, Wong CP. Silver nanoparticle-deposited boron nitride nanosheets as fillers for polymeric composites with high thermal conductivity. Sci Rep 2016;6:9.
[199] Shahil KMF, Balandin AA. Graphene-multilayer graphene nanocomposites as highly efficient thermal interface materials. Nano Lett 2012;12:861–7.
[200] Goyal V, Balandin AA. Thermal properties of the hybrid graphene-metal nano-micro-composites: applications in thermal interface materials. Appl Phys Lett 2012;100.
[201] Shahil KMF, Balandin AA. Thermal properties of graphene and multilayer graphene: applications in thermal interface materials. Solid State Commun 2012;152:1331–40.
[202] Malekpour H, Chang KH, Chen JC, Lu CY, Nika DL, Novoselov KS, et al. Thermal conductivity of graphene laminate. Nano Lett 2014;14:5155–61.